International Journal of Multimedia and Ubiquitous Engineering
Vol.9, No.8 (2014), pp.267-276
http://dx.doi.org/10.14257/ijmue.2014.9.8.24

YCbCr Image Supported NIR Image Enhancement

Gwanggil Jeon

Department of Embedded Systems Engineering, Incheon National University
119 Academy-ro, Yeonsu-gu, Incheon 406-772, Korea
gjeon@incheon.ac.kr

Abstract

This paper proposes high resolution RGB image supported near infrared (NIR) image super resolution method. In general, NIR image has low resolution characteristics. To show small image on bigger screen, super resolution method is applied to generate bigger image to fit the display. As CCD camera take colors images with high resolution, therefore one many extract helpful features for NIR image super solution. The RGB image is converted to YCbCr image, then edge enhancement technique in each channel (Y, Cb, and Cr) is applied. To provide the best performance globally, we train a parameter, p. Simulation results indicate that the proposed method enhance conventional super resolution methods.

Keywords: *Sensor, super resolution, near infrared image, CCD image, YCbCr color space*

1. Introduction

An image sensor transforms an optical image into a digital signal. It is widely used in image devices such as digital camera. The CFA image from CCD camera passes demosaicking process, and the result image has three color components, red, green, and blue, therefore the output image is color one. Meanwhile, infrared is electromagnetic radiation with longer wavelengths than those of visible light. Therefore, human eyes are not able to perceive the signal. In general, the wavelength spectrum is 700 nanometers (nm) to 1 mm. Generally, thermal radiation discharged by objects near room temperature is infrared. Figure 1 shows an example of infrared image.

Figure 1. An Example of Infrared Image

The near infrared (NIR) image has lower resolution. Since CCD camera can provide higher resolution image, one can generate higher resolution NIR image by adopting RGB image. To do so, we first transform RGB image into YCbCr image, and extract features from each component.

ISSN: 1975-0080 IJMUE

This paper proposes a concept of sensor fusion. Section 2 explains the proposed method. The training process of parameter p is determined. The proposed RGB image is concerted to YCbCr to extract features. Section 3 describes experimental results where objective and subjective performance are compared. Conclusion remarks are provided in Section 4.

2. Proposed Method: NIR Image Super Resolution

The image sensor fusion is a technique to merge sensory data different sources. In this paper, we assume two image sources, NIR image from infrared camera and RGB image from CCD camera. As RGB image has higher resolution, it is expected that RGB has more accurate edge information. The multi-sensor image fusion is a procedure of merging related information from two or more images into a single one. Therefore, the reconstructed image can show more informative and accurate image. As NIR images have lower resolution than that of RGB images, the resulting image of image fusion can give informative output image.

To conduct image sensor fusion, we first convert RGB image into YCbCr color space. YCbCr is an applicable approximation to color image processing and perceptual uniformity. YCbCr has component, luma signal (Y) and two chroma signals (Cb and Cr). Digital 8 bit YCbCr is derived from analog RGB as E. (1).

$$\begin{bmatrix} Y \\ Cb \\ Cr \end{bmatrix} = \begin{bmatrix} 16 \\ 128 \\ 128 \end{bmatrix} + \begin{bmatrix} 65.481R + 128.553G + 24.966B \\ -37.797R - 74.203G + 112.9B \\ 112.0R - 93.786G - 18.214B \end{bmatrix} \quad (1)$$

According to ITU-R BT.601, K_B and K_R have 0.114 and 0.299, respectively. Parameters K_B and K_R can be different. For example, ITU-R BT.709 indicate K_B and K_R are 0.0722 and 0.2126.

Figure 2 shows some examples of proposed idea. Figure 2(a) shows an original NIR image, which indicates NIR image has lower resolution. Figure 2(b) is RGB image with high resolution. Using Eq. (1), RGB image is concerted to YCbCr. Figure 2(c-e) are Y, Cb, and Cr images, respectively. Figure 2(f) is the output image. Figur3 shows the flowchart of our proposed method. Color space conversion is applied to obtain YCbCr image from RGB color space, and feature extraction is applied to Y, Cb, Cr components to help NIR LR image super resolution.

(a)

(b)

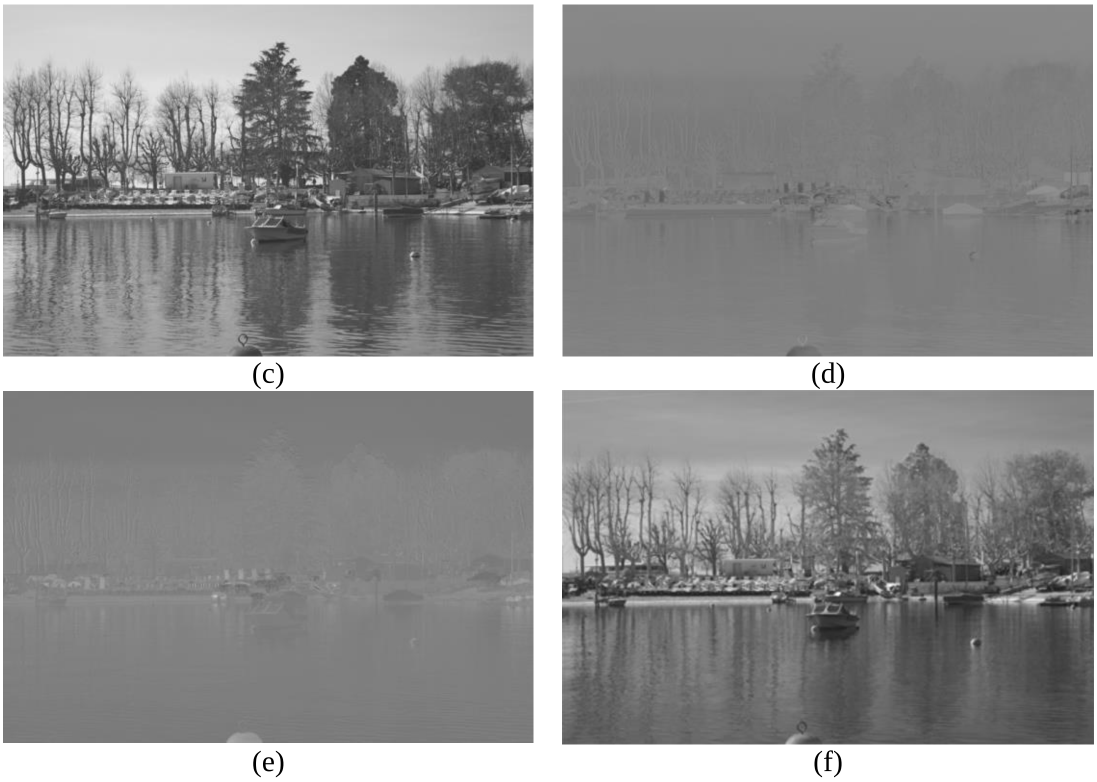

Figure 2. The 10th image of Zahra imageset: (a) low resolution NIR image, (b) high resolution RGB image, (c) Y component of RGB image, (d) Cb component of RGB image, (e) Cr component of RGB image, and (f) enhanced high resolution NIR image

In this paper, we assume three conventional super resolution methods: nearest neighbor method (NN), bilinear method (BI), and bicubic method (CU). To show the superiority of our proposed method on conventional ones, we compare both images in Fig. 4. All images show the difference between original images and restored ones. All images in left side show conventional NN (a), BI (b), and CU (c). On the other hand, all images in right side are color space conversion and feature extracted applied results. It can be found that the proposed method is useful to enhance the upsampled images.

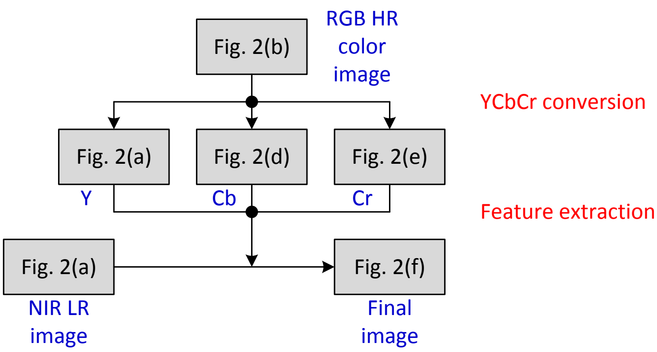

Figure 3. Flowchart of the Proposed Method to Obtain Final High Resolution NIR Image

The conventional NN, BI, and CU results are obtained as Eq. (2)

$$
\begin{aligned}
im_{NN}^{con} &= imfilter\left(INR, h_{NN}\right),\\
im_{BI}^{con} &= imfilter\left(INR, h_{BI}\right),\\
im_{CU}^{con} &= imfilter\left(INR, h_{CU}\right),
\end{aligned}
\tag{2}
$$

where h_{NN}, h_{BI}, h_{CU} are

$$
h_{NN} = \begin{bmatrix} 1 & 1 & 0 \\ 1 & 1 & 0 \\ 0 & 0 & 0 \end{bmatrix}, \quad
h_{BI} = \frac{1}{4}\begin{bmatrix} 1 & 2 & 1 \\ 2 & 4 & 2 \\ 1 & 2 & 1 \end{bmatrix}, \quad
h_{CU} = \frac{1}{64}\begin{bmatrix} 1 & 4 & 6 & 4 & 1 \\ 4 & 16 & 24 & 16 & 4 \\ 6 & 24 & 36 & 24 & 6 \\ 4 & 16 & 24 & 16 & 4 \\ 1 & 4 & 6 & 4 & 1 \end{bmatrix}. \tag{3}
$$

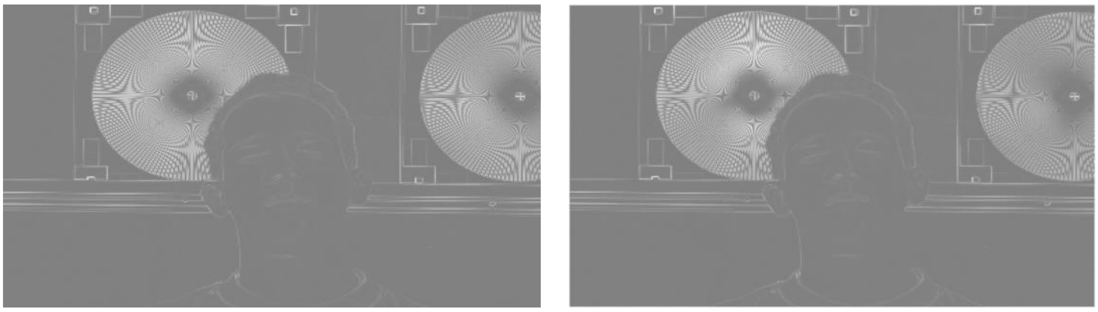

(a)

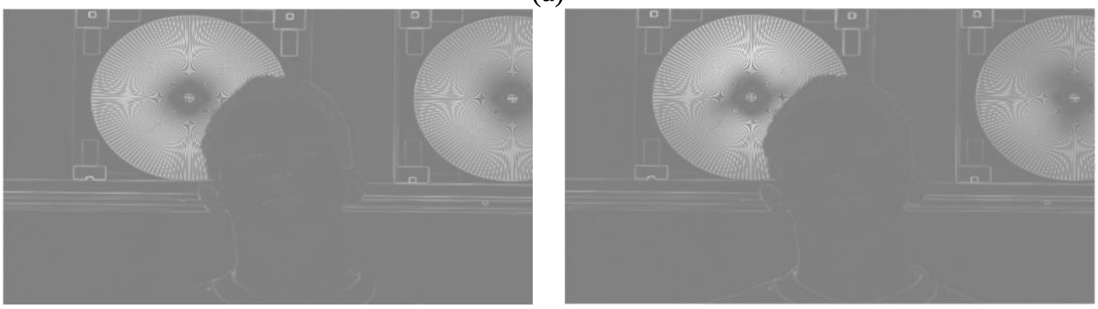

(b)

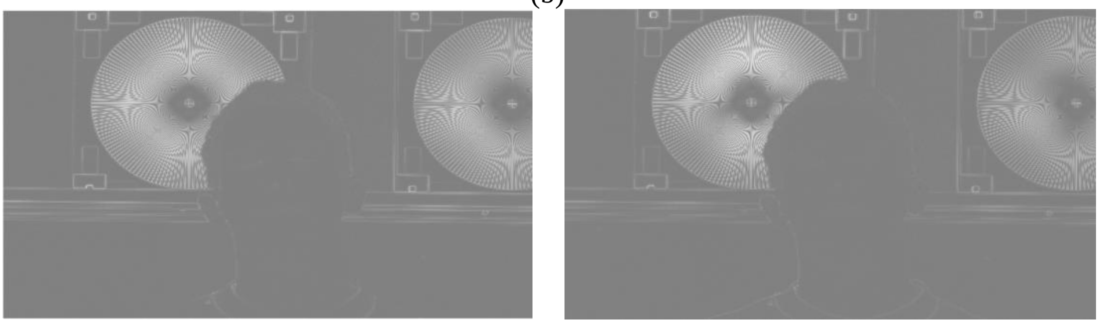

(c)

Figure 4. Left: difference between original image and conventional method. Right: difference between original image and high resolution YCbCr image supported conventional method applied image: (a) nearest neighbor, (b) bilinear, and (c) bicubic method

The proposed NN, BI, and CU results are obtained as Eq. (4)

$$\begin{aligned} im_{NN}^{con} &= imfilter(INR, h_{NN}) + \\ &\quad p \times \left\{ \frac{imfilter(Y, h_{HP}) + imfilter(Cb, h_{HP}) + imfilter(Cr, h_{HP})}{3} \right\}, \\ im_{BI}^{con} &= imfilter(INR, h_{BI}) + \\ &\quad p \times \left\{ \frac{imfilter(Y, h_{HP}) + imfilter(Cb, h_{HP}) + imfilter(Cr, h_{HP})}{3} \right\}, \\ im_{CU}^{con} &= imfilter(INR, h_{CU}) + \\ &\quad p \times \left\{ \frac{imfilter(Y, h_{HP}) + imfilter(Cb, h_{HP}) + imfilter(Cr, h_{HP})}{3} \right\}, \end{aligned} \tag{4}$$

where

$$h_{HP} = \begin{bmatrix} -1 & -2 & -1 \\ -2 & 12 & -2 \\ -1 & -2 & -1 \end{bmatrix}. \tag{5}$$

Parameter p can be determined empirically. Table 1 shows the performance results depend on various *p* values. Finally, *p* is determined as 0.0208.

Table 1. PSNR and MSE Results with Various Parameter *p*

p	Metrics	Nearest neighbor	Bilinear	Bicubic
0.0090	PSNR (dB)	26.8311	26.7141	27.9078
	MSE	134.8867	138.5708	105.2689
0.0095	PSNR (dB)	26.8397	26.7284	27.9211
	MSE	134.6215	138.1147	104.9478
0.0100	PSNR (dB)	26.8483	26.7423	27.9340
	MSE	134.3535	137.6730	104.6368
0.0120	PSNR (dB)	26.8764	26.7948	27.9773
	MSE	133.4874	136.0181	103.5987
0.0200	PSNR (dB)	26.9188	26.9373	28.0657
	MSE	132.1916	131.6290	101.5104
0.0208	PSNR (dB)	26.9168	26.9449	28.0660
	MSE	132.2509	131.3972	101.5045
0.0210	PSNR (dB)	26.9160	26.9463	28.0657
	MSE	132.2772	131.3571	101.5100
0.0230	PSNR (dB)	26.9052	26.9623	28.0598
	MSE	132.6043	130.8728	101.6487
0.0250	PSNR (dB)	26.8870	26.9684	28.0441
	MSE	133.1624	130.6896	102.0162
0.0300	PSNR (dB)	26.8105	26.9547	27.9657
	MSE	135.5271	131.1028	103.8755
0.0500	PSNR (dB)	26.1264	26.4704	27.1573
	MSE	158.6490	146.5684	125.1255
0.0800	PSNR (dB)	26.8131	26.6837	27.8806
	MSE	135.4468	139.5448	105.9313
0.1000	PSNR (dB)	23.1885	23.6384	23.7499
	MSE	312.0576	281.3476	274.2152
0.2000	PSNR (dB)	18.5813	18.7737	18.7246
	MSE	901.4742	862.3973	872.2062

3. Simulation Results

In this section, we present some experimental results. We compared our proposed method with conventional NN, BI, and CU methods. Figure 5 shows our tested imageset. There are 25 low resolution NIR images (Figure 5a) and their 25 corresponding high resolution RGB images (Figure 5b). Figure 5a is the training library to obtain *p*. These images were provided by Sadeghipoor *et al*. The details can be found in Figure 5.

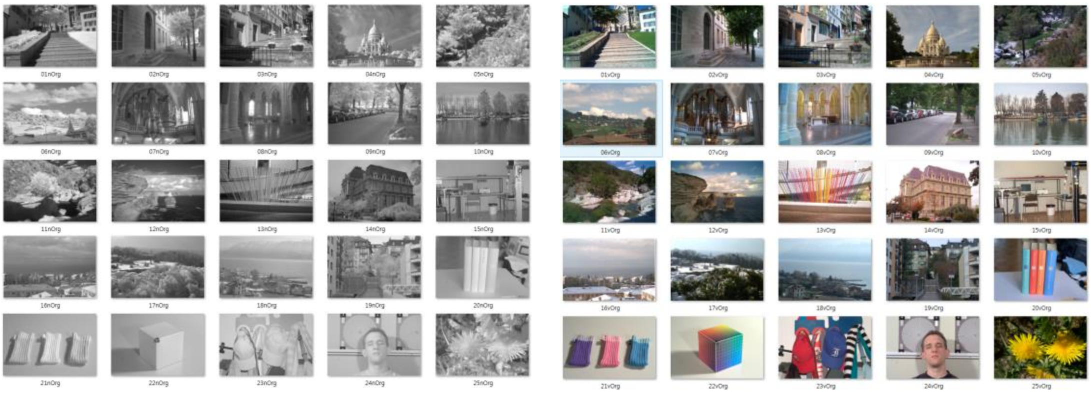

(a) (b)

Figure 5. Adopted Imageset: (a) NIR Zahra Imageset and (b) RGB Zahra Imageset

(a) (b)

Figure 6. Nearest Neighbor Case on 18th NIR Zahra image: (a) result image of conventional method and (b) HR YCbCr feature supported result image

Figure 6 compares subjective performance between conventional NN result image and proposed NN image. As it can be found, the proposed NN image gives better quality. Figures 7 and 8 show subjective performance of BI and CU cases. Figures 7(a) and 8(a) show conventional BI and CU results where we meet uncomfortable results. On the other hand, Figures 7(b) and 8(b) show proposed results, where unnecessary artifacts have been removed.

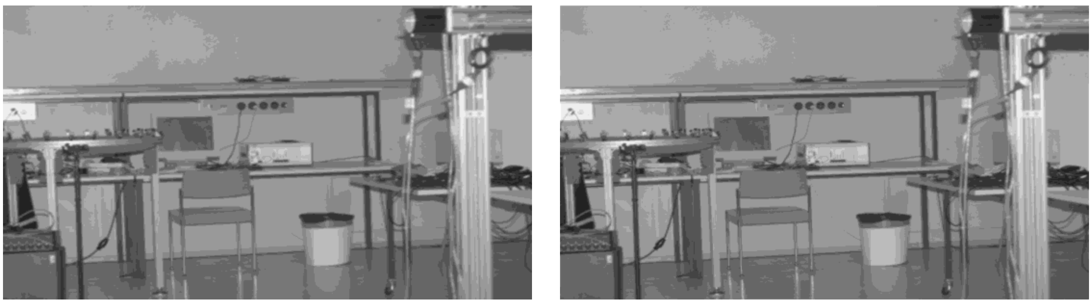

(a) (b)

Figure 7. Bilinear Case on 15th NIR Zahra image: (a) result image of conventional method and (b) HR YCbCr feature supported result image

(a) (b)

Figure 8. Bicubic case on 13th NIR Zahra image: (a) result image of conventional method and (b) HR YCbCr feature supported result image

Figures 9-11 show objective performance comparison in terms of PSNR (in dB) and MSE metrics. Used methods are NN, BI, and CU methods. Graphs in left side show PSNR case and graphs in right side indicate MSE case. From Figures 9-11, it can be found that the proposed approach raised objective performance significantly.

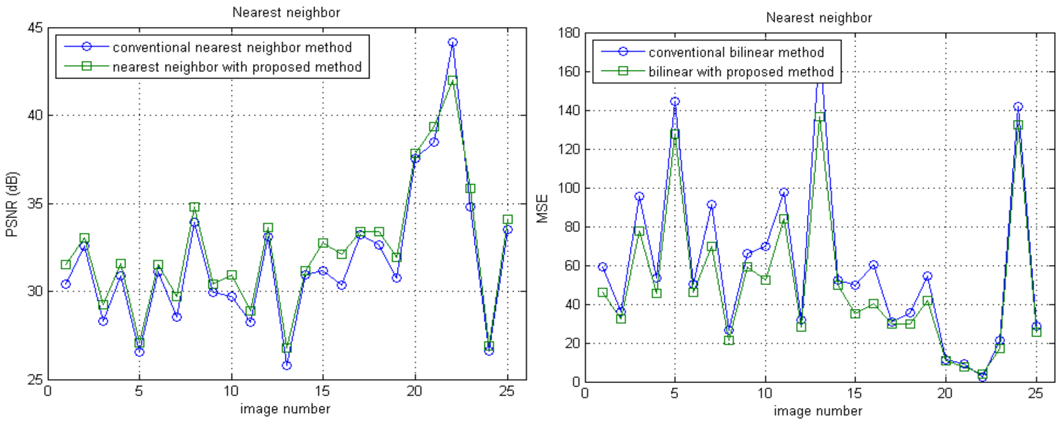

(a) (b)

Figure 9. Objective Performance Comparison in (a) PSNR and (b) MSE metrics for nearest neighbor method and the proposed method

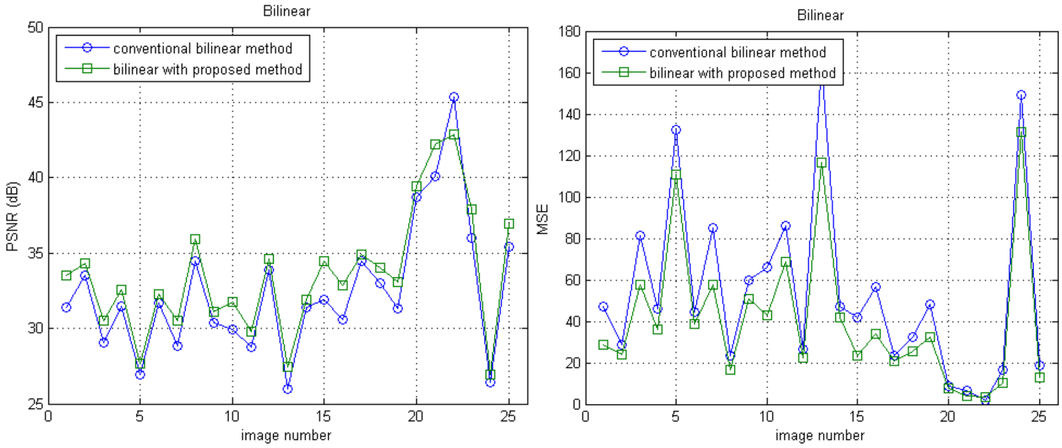

(a) (b)

Figure 10. Objective Performance Comparison in (a) PSNR and (b) MSE metrics for bilinear method and the proposed method

4. Conclusions

In this paper, we propose a new near infrared images upsampling approach using YCbCr color space information. Generally speaking, near infrared image shows lower resolution while CCA camera output image shows higher resolution. Since CCD camera image provides more information, one can use this information for near infrared images upsampling. Simulation results inform that the proposed method raised objective and subjective performances significantly.

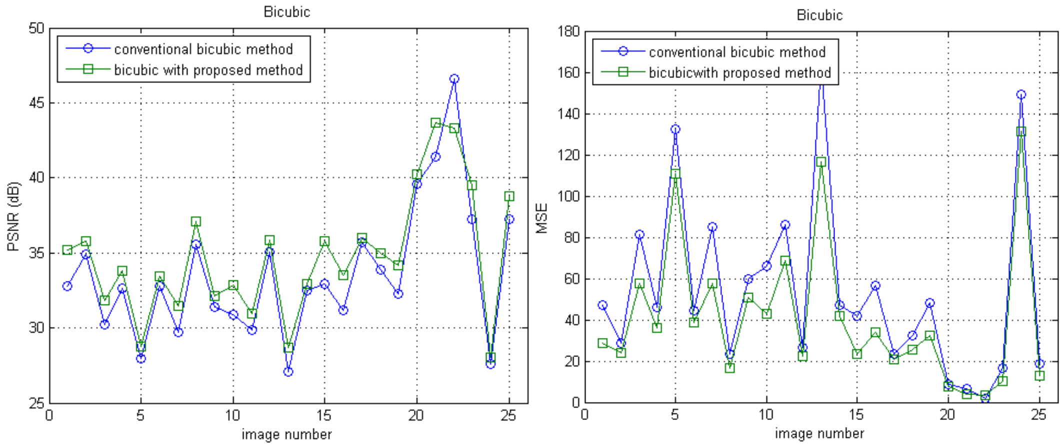

(a) (b)

Figure 11. Objective Performance Comparison in (a) PSNR and (b) MSE metrics for bicubic method and the proposed method

Acknowledgements

This research was supported by Basic Science Research Program through the National Research Foundation of Korea(NRF) funded by the Ministry of Science, ICT and Future Planning(2013R1A1A1010797)

References

[1] H. Li, B. S. Manjunath and S. K. Mitra, “Multi-sensor image fusion using the wavelet transform,” IEEE ICIP1994, vol. 1, (**1994**), pp. 51-55.
[2] H. Proença, “On the feasibility on the visible wavelength, at-a-distance and on-the-move iris recognition,” IEEE IEEE Symposium Series on Computational Intelligence in Biometrics: Theory, Algorithms, and Applications, (**2009**).
[3] J. G. Daugman, “New methods in iris recognition,” IEEE Transactions on Systems, Man, and Cybernetics - Part B: Cybernetics, vol. 37, no. 5, (**2007**), pp. 1167-1175.
[4] K. Park and J. Kim, “A real-time focusing algorithm for iris recognition camera,” IEEE Transactions on Systems, Man and Cybernetics, vol. 35, no. 3, (**2005**) August, pp. 441-444.
[5] L. Ma, T. Tan, Y. Wang and D. Zhang, “Local intensity variations analysis for iris recognition,” Pattern recognition, vol. 37, no. 6, (**2004**), pp. 1287-1298.
[6] Y. He, J. Cui, T. Tan and Y. Wang, “Key techniques and methods for imaging iris in focus,” in Proceedings of the IEEE International Conference on Pattern Recognition, (**2006**) August, pp. 557-561.
[7] J. R. Matley, D. Ackerman, J. Bergen and M. Tinker, “Iris recognition in less constrained environments,” Springer Advances in Biometrics: Sensors, Algorithms and Systems, (**2007**) October, pp. 107-131.
[8] J. G. Daugman, “How iris recognition works,” IEEE Transactions on Circuits and Systems for Video Technology, vol. 14, no. 1, (**2004**) January, pp. 21-30.
[9] . L. Cambier, “Iridian large database performance,” Iridian Technologies, Tech. Rep., (**2007**), http://iridiantech.com.

Author

Gwanggil Jeon received the BS, MS, and PhD (summa cum laude) degrees in Department of Electronics and Computer Engineering from Hanyang University, Seoul, Korea, in 2003, 2005, and 2008, respectively.

From 2008 to 2009, he was with the Department of Electronics and Computer Engineering, Hanyang University, from 2009 to 2011, he was with the School of Information Technology and Engineering (SITE), University of Ottawa, as a postdoctoral fellow, and from 2011 to 2012, he was with the Graduate School of Science & Technology, Niigata University, as an assistant professor. He is currently an assistant professor with the Department of Embedded Systems Engineering, Incheon National University, Incheon, Korea. His research interests fall under the umbrella of image processing, particularly image compression, motion estimation, demosaicking, and image enhancement as well as computational intelligence such as fuzzy and rough sets theories.

He was the recipient of the IEEE Chester Sall Award in 2007 and the 2008 ETRI Journal Paper Award.